DTIC FILE COPY

Contract N00014-86-K-0753

AD-A188 682

Development of Metastable Processing Paths for High Temperature Alloys

Craig Ward

Annual Technical Report
submitted to
Defense Advanced Research Projects Agency (DoD)
for the period
February 9, 1987 through September 30, 1987

Contractor: Metallurgy Division
National Bureau of Standards
Gaithersburg, MD 20899

Principal Investigator: William J. Boettinger
301-975-6160

Senior Project Scientists: Leonid A. Bendersky
Benjamin A. Burton
John W. Cahn
Robert J. Schaefer

Effective Date of Contract: February 9, 1987

Contract Expiration Date: December 31, 1989

Amount of Contract: $600,000

ARPA Order Number: 6065

Program Code Number: 7D10

DTIC
ELECTE
DEC 04 1987
S D
H

DISTRIBUTION STATEMENT A
Approved for public release;
Distribution Unlimited

87 11 5 003

Table of Contents

DTIC COPY INSPECTED

Accession For
NTIS GRA&I
DTIC TAB
Unannounced
Justification
By per letter
Distribution/
Availability Codes
Dist | Avail and/or Special
A-1

Summary

The possibility of developing new processing strategies for high temperature intermetallic compounds is being investigated. In particular rapid solidification followed by controlled heat treatment may provide new and unusual microstructures of multiphase materials. This report describes research performed at NBS to develop predictive models for solubility extension and metastable phase formation of intermetallic compounds and research to improve the phase diagram modeling of systems involving ordered phases.

Theory has been clarified to treat the interface shape stability for intermetallic compounds during solidification. Using modified variables to describe the phase diagram near an intermetallic compound the solidification conditions required to avoid microsegregation have been obtained.

Experimental research has been conducted on three intermetallic systems, Al_3Nb, NiAl-NiTi, and TiAl to gain an experimental data base for theoretical model development using melt spinning and examination by transmission electron microscopy. In the case of Al_3Nb, which is considered a line compound, solubility extension was not obtained by melt spinning, although a thermodynamic analysis suggests that such extension is possible. In the NiAl-NiTi system, the equilibrium intermediate Heusler phase, Ni_2AlTi, was suppressed by rapid solidification and extension of the composition range of the NiAl and NiTi phases was observed. Solid state decomposition of these supersaturated phases occurs by continuous ordering into the Heusler phase and subsequent spinodal decomposition into a two-phase mixture of NiAl + Ni_2AlTi or NiTi + Ni_2AlTi depending on composition. In the TiAl system rapid

solidification was found to suppress the formation of the TiAl phase, at least as the primary solidification phase. A disordered hexagonal phase was found to form from the liquid in melt-spun ribbons. The subsequent solid state ordering and decomposition of this phase was documented. In general, these results indicate that significant modifications in microstructure are possible using unconventional processing methods. The precise limitations of these microstructural modifications are being defined and a theoretical basis for prediction is being sought.

I. Introduction

The development of high temperature materials is closely related to the formulation of processing strategies for chemically ordered phases. Most intermetallic compounds including aluminides, carbides, and silicides as well as high temperature ceramic phases are ordered. However, optimum mechanical properties are likely to come from intimate dispersions of several phases, some of which are ordered. These dispersions can be produced by a phase transformation sequence involving both ordering and phase separation beginning with a solid phase of a carefully selected unstable composition made by rapid solidification.

Recently, significant advances have occurred in the utilization and understanding of rapid solidification processing of alloys. Factors which promote refined segregation, solubility extension and metastable phase formation have been identified. However, much of this research has been focused towards disordered crystalline phase: i.e., terminal solid solutions, not ordered intermetallic compounds.

At the same time, significant advances have been realized in thermodynamics and kinetics of order-disorder transitions. The distinction between first and higher order transitions has been clarified, the kinetics of ordering reactions and the structure and mobility of APB's have been determined and reactions that involve fine scale ordering and compositional separation have been studied.

This research attempts to combine the advances in these areas to develop new processing strategies for high temperature ordered multiphase materials.

In this research we intend to define those experimental results which are within the scope of current understanding and to explore those results which demand modification of current theory.

A brief example of the interrelation between order-disorder processes and rapid solidification might be in order. The possibility of creating a disordered intermetallic compound with extended solubility would provide unique opportunities for the development of multiphase structures by subsequent heat treatment. Somewhat surprisingly in some cases rapid solidification naturally favors the formation of the ordered phase. In other cases thermodynamic factors or nucleation and growth kinetic limitations prevent the formation of the ordered phase directly from the melt and a disordered phase can form from the melt. These kinetic factors require investigation.

Retention of the disordered phase on cooling in the solid state depends on the kinetics of the ordering processes. Ordering can occur continuously throughout the grains or by nucleation and growth of ordered regions. The former is usually quite fast and the latter is more sluggish because long range diffusion is required. To distinguish which occurs, it is important to recognize that many disordered phases have limits to the metastability; i.e., below a certain temperature they become unstable and spontaneously order. Such limits are usually termed spinodals. The position of these spinodals can be estimated by appropriate thermodynamic modeling. At compositions and temperatures above these spinodals, ordering transitions must occur by nucleation and growth. Thus, alloys in which disordered structures can be retained on quenching can be identified. The position of these spinodal

curves, as well as spinodals associated with compositional phase separation also define possibilities for subsequent heat treatment and microstructural stability of multiphase alloys at high temperature.

In Section II of this report we describe research focused on determining the possibility of extending the solubility range of ordered phases by rapid solidification. Subsequent heat treatment of these metastable alloys can form stable high temperature multiphase mixtures. This research also includes an examination of the state of nonequilibrium order of rapidly quenched intermetallic compounds.

Section III of this report describes efforts focused on increasing phase diagram modeling capability where ordered phases are involved. This includes the use of Bragg-Williams and Cluster Variation Methods (CVM) to model phase boundaries between ordered and related disordered phases like α-Ti and Ti_3Al as well as between related ordered phases like NiAl and Ni_2AlTi.

The appendix consists of preprints of manuscripts accepted for publication which have resulted from this research.

II. Solubility Extension of Ordered Phases by Rapid Solidification

An interesting class of microstructures recently being considered to increase the ductility of brittle phases consists of ductile particles embedded in a hard matrix. One potential processing path to form such a microstructure is to gain extension of the range of solubility of an ordered phase in the composition direction of a ductile equilibrium phase. Subsequent heat treatment would then form particles of the ductile phase in the ordered matrix. We examine the conditions under which the solubility range of ordered phases can be extended by rapid solidification.

Intermetallic ordered phases fall into two categories: those which exist over a relatively wide composition range and those which have a relatively narrow range of stability (line compounds). Examples of the former are Ni_3Al, TiAl, Nb_3Al while very narrow ranges occur for phases such as Al_3Ti, Al_3V, and Al_3Nb. Theory indicates that the consequences of the rapid solidification of these two categories are quite different. Ordered phases with wide equilibrium solubility ranges are often preferred for alloy development. However, the high temperature stability or resistance to coarsening of two phase mixtures when the matrix phase has a narrow equilibrium solubility range should be good. Thus a study of both types of phases is important.

For terminal solid solutions, extension of solid solubility occurs by two mechanisms: (1) avoidance of a stable eutectic or peritectic second phase due to nucleation and growth difficulties and as a consequent; solidification of the primary phase on the metastable extensions of the

liquidus and solidus, and (2) nonequilibrium solute trapping of the alloying additions at levels exceeding the solidus (whether stable or metastable). In both cases, of course, a smooth planar interface must be morphologically stable or dendritic microsegregation will occur. For line compounds significant solubility extension cannot occur by mechanism 1 because the extended solidus does not offer significant composition change (Figure 1). Thus solubility extension must occur by mechanism 2. For ordered phases with a range of composition both mechanisms can yield solubility extension.

In order to gain insight into these questions we have:

(a) Theoretically examined the conditions for the solidification of intermetallic compounds with a smooth (planar) interface. A smooth interface avoids microsegregation.

(b) Experimentally examined the effect of melt spinning on the possible range of nonequilibrium composition of the DO_{22} phase based on Al_3Nb.

(c) Experimentally examined the microstructure of alloys between NiAl and NiTi.

(d) Performed TEM examination of melt spun ribbons of composition near TiAl in collaboration with Professor J. Perepezko, University of Wisconsin, in support of work under DARPA sponsorship.

The results of the investigation are summarized below. For items (c) and (d) preprints of papers based on this research can be found in the appendix.

(a) Planar Interface Stability During the Solidification of an Intermetallic Compound

The results of the general theory for interface shape stability are usually given in a form that assumes that the liquidus and solidus lines are

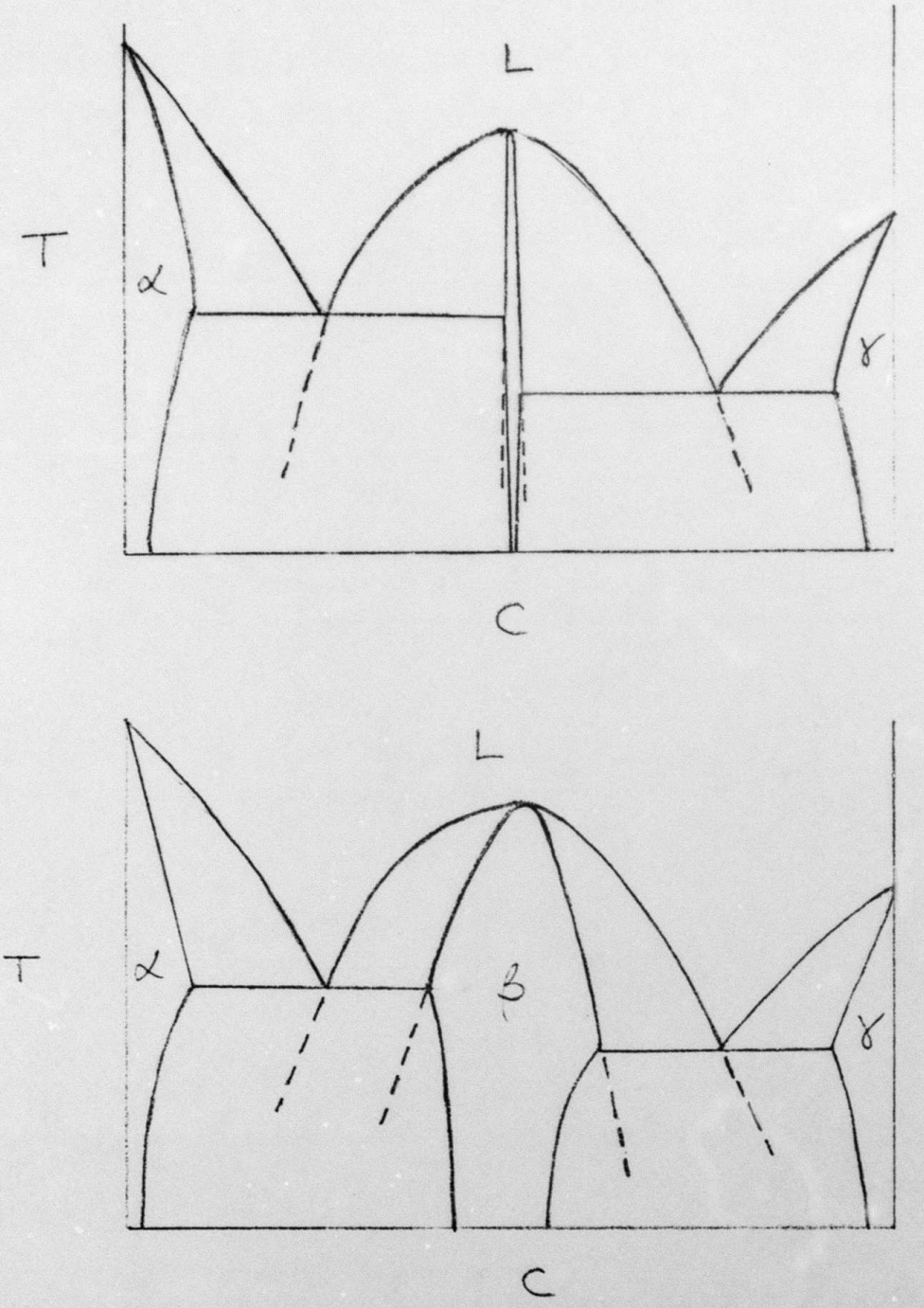

Figure 1. Schematic phase diagram of eutectic system involving an intermetallic compound β with (top) a narrow range of solubility and (bottom) a wide range of solubility. Metastable solidification of the β phase in the absence of α and γ is shown by the dashed lines. Little solubility extension of β is possible by this mechanism in the top.

straight. For intermetallic compounds these curves are typically curved, especially near a maximum in the liquidus (see Figure 1).

An examination of the scientific literature revealed a recent paper (C. Misbah, J. de Physique 47 (1986) 72) which correctly treats this question for the case where local equilibrium is maintained across the liquid solid interface and where the liquidus, T_L, and solidus, T_S, can be represented by parabolic arcs as a function of liquid and solid compositions, C_L and C_S, as

$$T_L = T_M + \alpha_L (C_L - C_M)^2$$
$$T_S = T_M + \alpha_S (C_S - C_M)^2$$

T_M and C_M are the temperature and composition of the congruent maximum (or minimum) in the liquidus and solidus curves and α_L and α_S are constants. By defining new composition variables,

$$\tilde{C}_L = C_L - C_M$$
$$\tilde{C}_S = C_S - C_M$$

a constant equilibrium partition coefficient, k, can be defined by the usual ratio given by

$$k = \frac{\tilde{C}_S}{\tilde{C}_L} = \sqrt{\frac{\alpha_L}{\alpha_S}}$$

and a liquidus slope, m, which is not constant but depends on solid composition as

$$m = 2\tilde{C}_S \alpha_L / k.$$

The results of the Misbah theory can be simply seen for this case by substituting the new composition variable and values for m and k as defined above into the usual theory for straight liquidus and solidus curves; i.e., for absolute stability the velocity v is given by

$$v > \frac{mD_L(1 - k)\tilde{C}_o}{k^2 T_M \Gamma}$$

where D_L is the liquid diffusion coefficient, $\tilde{C}_o$ is the alloy composition in the new composition coordinate and $T_M\Gamma$ is the capillary constant.

Thus the condition for stability of a planar interface for an intermetallic compound can be calculated in a straightforward manner. One might note that for some phases such as TiAl the congruent maximum would be metastable but values of T_M and C_M would be found to fit the liquidus and solidus data where they exist.

(b) Solubility Extension of a Line Compound

Alloys of composition Al-22 at% Nb and Al-28 at% Nb were prepared by arc melting. These alloys were ± 3 at% on either side of the compound Al_3Nb. Alloys were melt spun on a Cu wheel in a He atmosphere. The produced ribbons were electropolished and examined by transmission electron microscopy. Neither composition was single phase indicating that solubility extension, if present, was less than 3 at%. The Al-22 at% Nb ribbon microstructure consists of cells of the Al_3Nb phase surrounded by FCC aluminum phase. The Al-28 at% Nb ribbons consist of cells of the Al_3Nb phase surrounded by the σ(Al,Nb) phase. Both are the expected equilibrium structures given by the phase diagram (Figure 2).

Although these initial attempts to extend the solubility of a line compound by rapid solidification were unsuccessful, future work is planned with alloys closer to stochiometry and using higher cooling rates.

(c) Solubility Extension in the NiAl-NiTi Systems

Alloys belonging to the quasi-binary system containing NiAl, Ni_2AlTi, and NiTi were chosen for a study of solubility extension of intermetallic

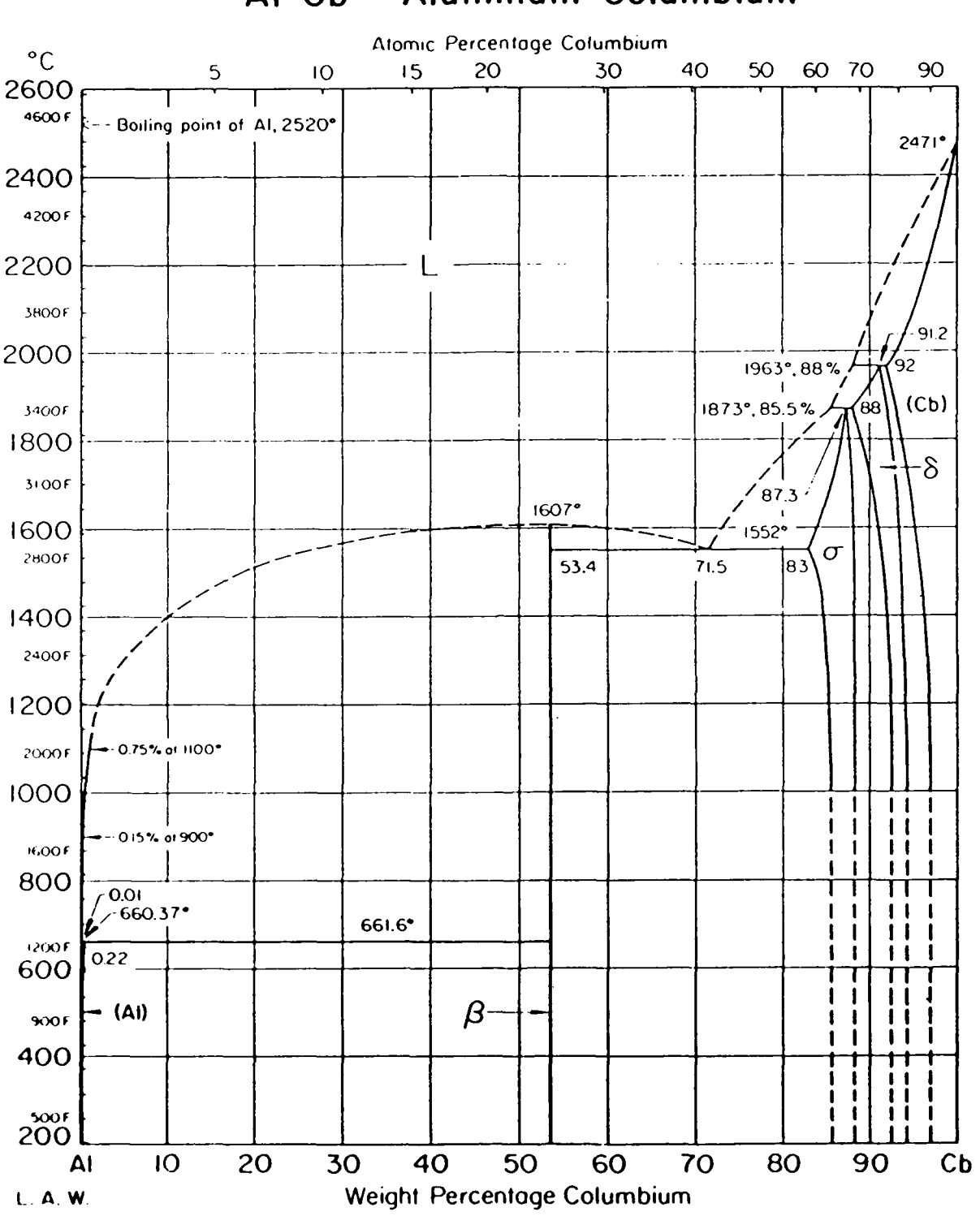

Figure 2. Al-Nb phase diagram. The phase labeled β is Al_3Nb with DO_{22} structure.

compounds with significant equilibrium ranges of solubility. This specific alloy system was also chosen because Heusler phase based on the ideal composition Ni_2AlTi(NiAl•NITi) has a crystal structure, $L2_1$ (identical to DO_3), which is an ordered form of the B2 structure. Although the solid state B2 to DO_3 transformation satisfies the Landau rules for an allowable higher order transition, the system contains a pair of two phase fields, NiAl + Ni_2AlTi and Ni_2AlTi + NiTi, indicating that the transition is first order at those temperatures. These two-phase fields permit the study of solubility extension by rapid solidification and an exploration of nonequilibrium ordered states and reaction paths.

The results of the rapid solidification experiments are described in detail in the preprint contained in the appendix. Briefly the solubility range of the B2 phases, NiAl and NiTi, were increased. More Ti was forced into the NiAl phase and more Al into NiTi phase than can be obtained by conventional solidification or solution heat treatment. This suggests a kinetic preference for the formation of the B2 phases over the $L2_1$ phase (Ni_2AlTi).

Solid state transformations are quite rapid in this alloy system. The supersaturated B2 orders continuously into single phase $L2_1$ during the solid state cooling of the melt spinning process. Subsequent heat treatment develops two phase microstructures of B2 + $L2_1$. The kinetics of this process are being studied in more detail.

(d) <u>The Microstructure of Rapidly Solidified and Heat Treated Alloys Near the TiAl Composition</u>

Alloys based on the $L1_0$ phase of the Ti-Al system near TiAl are currently being considered for low density, high temperature applications.

These alloys may ultimately be used in a form consisting of mixtures of phases such as TiAl with Ti_3Al ($\gamma + \alpha_2$) or TiAl with a BCC phase ($\gamma + \beta$) when Nb is added. Also composites, which may use atomized powders of TiAl, are of interest.

We have examined the microstructure of rapidly solidified melt spun ribbons of alloys between Ti-52 at% Al and Ti-54 at% Al. This work has been performed in close collaboration with Professor John Perepezko under DARPA/URI sponsorship and complements his research on rapidly solidified powders. The results are reported in detail in the preprint in the appendix.

Briefly, as-solidified melt spun ribbons were found to contain a dendritic structure of one phase surrounded by a matrix phase. The dendritic phase was the ordered hexagonal phase with DO_{19} structure (α_2). The dendrites contain fine antiphase domains indicating that the ordered phase did not form direclty from the liquid phase but formed by a solid state reaction. A reasonable conclusion is that the disordered hexagonal (α) phase formed during rapid solidification. The matrix phase in the ribbon structure was the $L1_0$ structure (γ) based on ordered TiAl.

The ribbons contained some indication of further solid state transformation. The α_2 structure at these compositions is supersaturated and must eventually decompose to a mixture of α_2 and γ. This transformation takes place by the formation of stacking faults in the DO_{19} phase. These faults locally transform the hexagonal stacking into a FCC stacking. These regions provide the nucleus for plates of the $L1_0$ (γ) phase. The transformation continues by thickening of the γ plates at the expense of the α_2 phase. In heat treated ribbons this process converts the hexagonal phase formed during solidification completely into γ phase.

III. Advanced Phase Diagram Modeling

There has always been a significant gap between the efforts of phase diagram modelers and measured phase diagram data. First principle approaches do not presently have great usefulness for the development of unique processing strategies. However, significant advances have recently occurred for phase diagram modeling using another approach. Existing phase diagram and thermodynamic data, which often exist only in limited composition or temperature ranges, can be fitted using free energy functions based on reasonable physical models of phases with adjustment of parameters which relate to these physical models. Although phase diagrams based on such modeling can never replace carefully measured diagrams, they do provide a thermodynamically consistent first approximation to the equilibrium diagram. They provide two types of information. Choices of composition and temperature can be determined for critical experiments which minimize the number of alloys prepared. Qualitative features of metastable phase diagrams can be used to guess general processing strategies for specific alloy systems without a knowledge of the precise location of phase boundaries.

For ordered intermetallic phases three methods are available for modeling the free energy and hence phase diagrams. Landau expansions are useful to determine qualitative features of phase transformation near critical points. Sublattice or Bragg-Williams models are useful for describing phases where the difference in size, charge or electronegativity causes a deviation from random mixing of the atoms; i.e., the formation of long range order. It treats the phase like a regular solution with a number of sublattices. The third method involves the calculation of free energies

by summing the energy of clusters of atoms (usually tetrahedral or octahedral) and is called the cluster variation method.

A great majority of ordered structures which are considered useful as structural materials are based on ordering of BCC, FCC, and HCP lattices. In the research performed under this contract we intend to focus on the modeling of ordered phases in ternary alloys based on these three basic lattices. Real phase diagrams will be a superposition of these with one type being dominant over some range of composition and/or temperature.

Initial efforts are being focussed on ternary alloys based on the BCC lattice. A Bragg-Williams or sublattice approach has been used to model the quasi-binary section between NiAl and Ni_2AlTi in the Ni-Al-Ti ternary system. This system was chosen to support the experimental program described in Section IIc but also because of the strong crystallographic (and hence thermodynamic) relation between the B2(NiAl and NiTi) and $L2_1$(Ni_2AlTi) structures. The $L2_1$ structure is an ordered form of the B2 structure. This relationship is reflected in the metastable tricritical point between the B2 and $L2_1$ phases shown in Figure 3. Measurements are underway to define the proper choice of thermodynamic parameters. Future work will be focused on modeling a full ternary BCC phase diagram with these kinds of ordered structures.

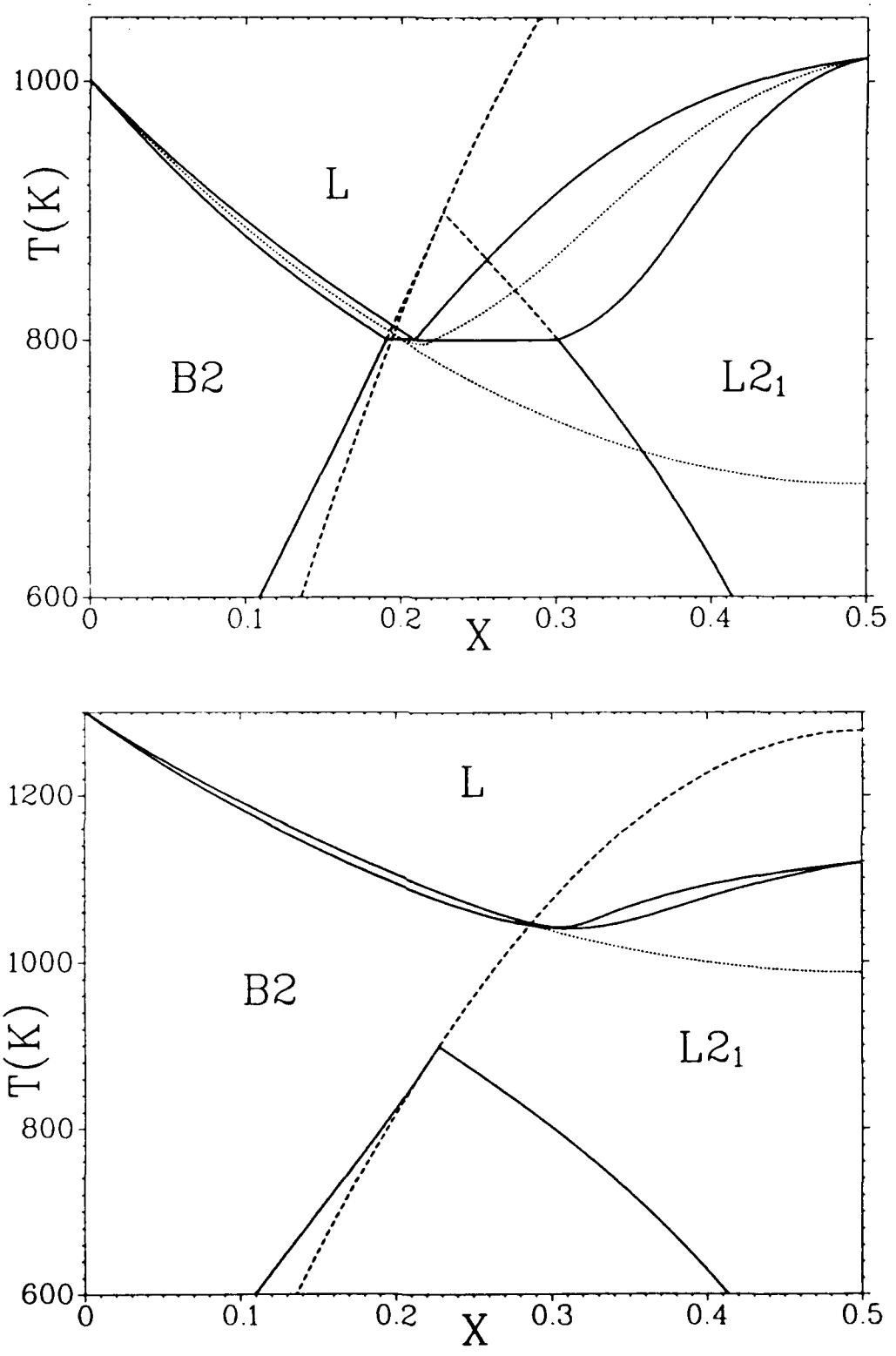

Figure 3. Bragg-Williams model of the quasi-binary section between NiAl(X = 0) and Ni_2AlTi(X = 0.5) using different values of the thermodynamic parameters. NiAl has the B2 structure and Ni_2AlTi has the $L2_1$ structure. At the top the two phase region between B2 and $L2_1$ intersects the liquidus, while at the bottom the two phase region is below the liquidus.

Appendix - Preprints of Manuscripts

preceding page blank - not filmed

Proceedings of RQ6, Montreal, August 1987
to appear in Mat. Sci. and Eng., 1988

Rapid Solidification and Ordering of B2 and $L2_1$ Phases in the NiAl-NiTi System

W. J. Boettinger, L. A. Bendersky, F. S. Biancaniello, J. W. Cahn

Institute for Materials Science and Engineering
National Bureau of Standards
Gaithersburg, MD 20899

Abstract

Evidence is presented for the direct solidification of the B2 phase in the NiAl-NiTi system at some compositions where the $L2_1$ phase is stable at the melting point. Subsequent continuous ordering produces the equilibrium phase. The metastable continuous ordering curve is used to discuss this result.

Introduction

Rapid solidification of intermetallic compounds may result in reduction of microsegregation, extension of solubility, and manipulation of long range order or antiphase domain (APD) size. The mechanisms responsible for observed variations in domain size (1-3) are not well understood. The microstructural modifications made possible by rapid solidification can permit the development of new and unusual two-phase structures during subsequent heat treatment.

Many technologically important ordered phases are closely related to disordered cubic or hexagonal structures which also occur in the same system. This crystallographic relationship between phases has important implications for the thermodynamics of these phases and the mechanisms of phase formation that must

be considered to determine the various options which are available during processing.

In the present paper we report the microstructure of melt spun alloys with compositions between the B2 phases, NiAl and NiTi. This system was chosen for study because of the existence of a ternary Heusler phase based on the ideal composition Ni_2TiAl (NiAl·NiTi) (4). Its crystal structure, $L2_1$ (identical to DO_3), is an ordered form of the B2 structure. Although the solid state B2 to DO_3 transformation satisfies the Landau rules for an allowable higher order transition, the system contains a pair of two phase fields, NiAl + Ni_2AlTi and Ni_2AlTi + NiTi (4,5,6), indicating that the transition is first order at those temperatures. These two-phase fields permit the study of solubility extension by rapid solidification and an exploration of nonequilibrium ordered states and reaction paths.

Experimental Procedure

Alloys were prepared by the arc melting of 99.99% pure components. All alloys contained 50 at% Ni and the following Ti contents with the balance being Al: 7.5, 12.5, 15, 17.5, 20, 25, 37.5, and 45 at% Ti. Arc melted ingots were examined by standard optical metallography and by SEM. Rapidly solidified samples were prepared by melt spinning in He on a Cu wheel. TEM samples were prepared by twin jet electropolishing in 8% perchloric in acetic acid at room temperature.

Phase Diagram

Kaufman and Nesor (7) calculated the Ni-Al-Ti ternary assuming the Heusler phase was a line compound. Nash and Liang

(6) give an isothermal section at 900°C showing a significant solubility range for Ni_2TiAl and a liquidus projection. According to the calculation of Kaufman and Nesor, only the region between NiTi and Ni_2TiAl is quasibinary (section contains all tie lines). The liquidus of Nash and Liang implies that only the region between NiAl and Ni_2TiAl is quasibinary.

Results

Arc Melted Samples

Of particular interest for the interpretation of the rapid solidification results are the character of the invariant reactions (eutectic or peritectic) and the equilibrium solubility limits of the NiAl, Ni_2AlTi, and NiTi phases. Microprobe and TEM analysis was used to determine the primary and secondary phases in the arc melted samples. These results are summarized in Table 1. Microprobe results were also interpreted to give the solid solubility limits of the phases near their respective invariants: NiAl, 0 to 11 at% Ti; Ni_2TiAl, 18 to 29 at% Ti; and NiTi 42 to 50 at% Ti. Our results are consistent with the notion of a quasibinary, except at high Ti where we found $NiTi_2$.

Ribbons

The microstructure of the ribbons generally consists of columnar grains with diameters between 1-5 μm which extend across the ribbons. Figure 1a shows a nonuniform cored structure within a grain in a 12.5 at% Ti alloy. The centers have the B2 structure, are low in Ti, and contain fine $L2_1$ precipitates; the outsides have the $L2_1$ structure, are high in Ti, and contain fine

APD's. A 7.5 at% Ti alloy is similar except the centers are free of precipitates. This non-uniform structure is the result of cellular solidification and the resulting microsegregation of Ti to the cell boundaries expected for the crystallization of NiAl according to the phase diagram to be described below. Alloys containing 17.5 at% Ti sometimes contained cells with similar segregation but also appeared with a relatively uniform APD size as shown in Figure 1b.

In alloys with intermediate levels of Ti (20, 25 at%) the structure is $L2_1$ with no cells but with a significantly larger APD size (Figure 2a). At 37.5 at% Ti the microstructure again consists of $L2_1$ grains but with a much smaller domain size (Figure 2b). A ribbon with 45 at% Ti contained grains of the B2 phase without any APD's.

The displacement $\underline{u}$ associated with the APB's was determined. In the B2 structure $\underline{u}$ can only be along [111] whereas in the $L2_1$ phase $\underline{u}$ can also be along [100]. Only [100] boundaries were found. The B2 regions and the $L2_1$ regions were free of [111] boundaries. Where $L2_1$ regions with <u>fine</u> domains occur, we infer that the B2 phase formed from the melt with the [100] APB's forming during solid state ordering to the $L2_1$ phase. Samples free of APB's are likely to result from direct solidification of the $L2_1$ phase. The coarse domains found in the 20 and 25 at% alloys could have resulted from either direct solidification of $L2_1$ or from such a high temperature ordering of the B2 phase that much domain growth occurred during the quench.

Table 1. Phases Present in Arc Melted Samples

Alloy Composition (at% Ti)	Primary Phase	Secondary Phases
7.5	NiAl	Heusler
12.5	NiAl	Heusler
15	NiAl	Heusler
17.5	Heusler	not determined
20	Heusler	NiAl
25	Heusler	not determined
37.5	Heusler	NiTi, $NiTi_2$
45	NiTi	not determined

Discussion

The results from the arc melted buttons as well as preliminary thermal analysis were used to estimate the quasibinary diagram in Figure 3, even though we have some evidence of segregation outside the quasibinary. The ribbon results indicate that rapid solidification increases the metastable range of compositions over which the B2 phase solidified directly from the melt to include compositions where the $L2_1$ phase is the equilibrium phase at the melting point. The formation of the more disordered phase by rapid solidification in this system is surprising and requires further study.

Figure 3 includes curves for the metastable extensions of the B2 + $L2_1$ two-phase fields above the liquidus and a curve for continuous ordering without a composition change. Such continuous ordering requires only short-range diffusion and should be fast compared to all other solid-state diffusional processes. The reader should refer to Allen and Cahn (8) for a

full discussion of continuous ordering within a two-phase field. One of the important questions in the present work is whether this line also defines which solid phase forms directly from the melt. With our present knowledge of the phase diagram, very little is known about the location of this curve, but it must be confined within the stable and metastable two-phase fields. The 17.5 at% Ti composition should be clearly on the $L2_1$ side at all temperatures where solid is stable. Therefore the observation of a fine domain size in a noncellular region of the 17.5 at% ribbons seems to indicate a solidification to B2 under conditions where $L2_1$ had to be the more stable phase, followed by subsequent ordering to $L2_1$. A similar situation may occur for the 37.5 at% Ti alloy.

In the study of the NiAl-Cr eutectic, rapid solidification produced the expected ordered B2 phase instead of the disordered bcc phase (9). The metastable construction using a tricritical point to locate the continuous ordering curve had indicated that the metastable range of the ordered phase should expand much more than that of the bcc phase. The construction for the NiAl-NiTi system is depicted in Figure 3. The T_o curve for the partitionless solidification to $L2_1$ terminates at the two points where it intersects the continuous ordering curves. In between, the T_o for $L2_1$ lies everywhere at a higher temperature than the T_o curve for solidification to B2. In this range of compositions during cooling, direct partitionless solidification to $L2_1$ becomes thermodynamically possible before it becomes possible to

form B2 without partitioning. However, in the 17.5 and 37.5 at% Ti alloys, as judged by the fine domains, B2 forms by partitionless solidification rather than $L2_1$ even though B2 requires greater undercooling.

For the alloys with compositions of 7.5 and 12.5 at% Ti, the centers of the cells have lower Ti contents. Thus in the 7.5 at% alloy after quenching to room temperature these centers may lie in the single phase NiAl region and can be retained. For the 12.5 at% Ti alloy, the cell centers likely have somewhat higher Ti levels and may fall just within the equilibrium NiAl + Ni_2TiAl two phase field but outside the ordering curve after quenching. Thus, decomposition of the B2 phase must occur by nucleation and growth of $L2_1$ precipitates causing the fine $L2_1$ particles in the cell centers in Figure 2b.

Acknowledgement

We thank C. Brady and A. Shapiro for analysis of the cast samples, R. S. Polvani for providing the Al-rich samples and B. Burton for helpful discussions. The support of DARPA is appreciated.

References

1. A. Inoue, T. Masumoto, H. Tomioka and N. Yano, Inter. J. Rapid Solidification 1 (1984) 115.

2. S. C. Huang, E. L. Hall, K. M. Chang and R. P. Laforce, Met. Trans. 17A (1986) 1685.

3. C. C. Koch, J. A. Horton, C. T. Liu, O. B. Cavin and J. O. Scarbrough, in Rapid Solidification Processing: Principles and

Technologies III, R. Mehrabian, ed., NBS (1982) p. 264.

4. A. Taylor and R. W. Floyd, J. Inst. Metals 80 (1952-3) 25.

5. R. S. Polvani, W. S. Tzeng and P. R. Strutt, Met. Trans 7A (1976) 33.

6. P. Nash and W. W. Liang, Met. Trans. 16A (1985) 319.

7. L. Kaufman and H. Nesor, Met. Trans. 5 (1974) 1623.

8. S. M. Allen and J. W. CAhn, Acta Met. 24 (1976) 425.

9. W. J. Boettinger, D. Shechtman, T. Z. Kattamis and F. S. Biancaniello, Acta Met. 32 (1984) 749.

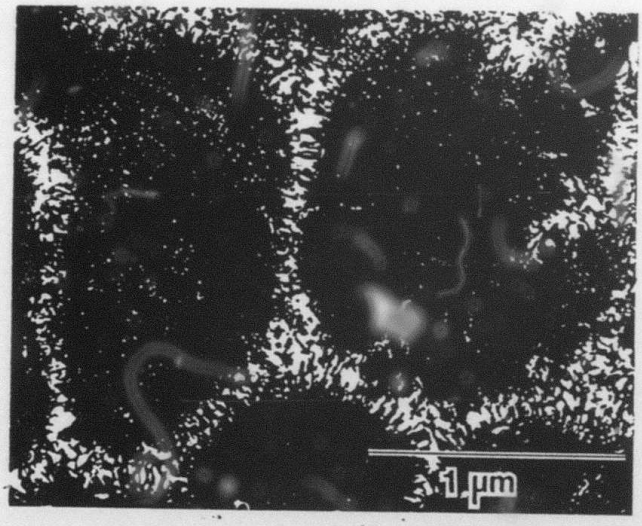

a

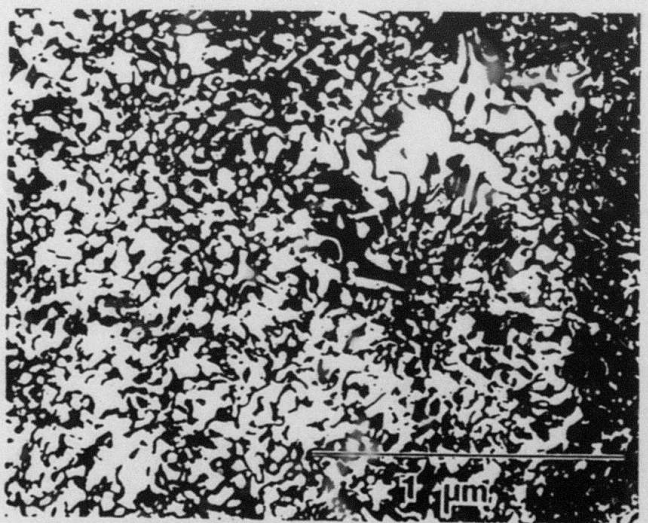

b

Figure 1 (a) (b). Dark field TEM micrographs using (111) $L2_1$ superlattice reflection of melt-spun ribbons of (a) Ni-12.5 at% Ti-37 at% Al and (b) Ni-17.5 at% Ti-32.5 at% Al.

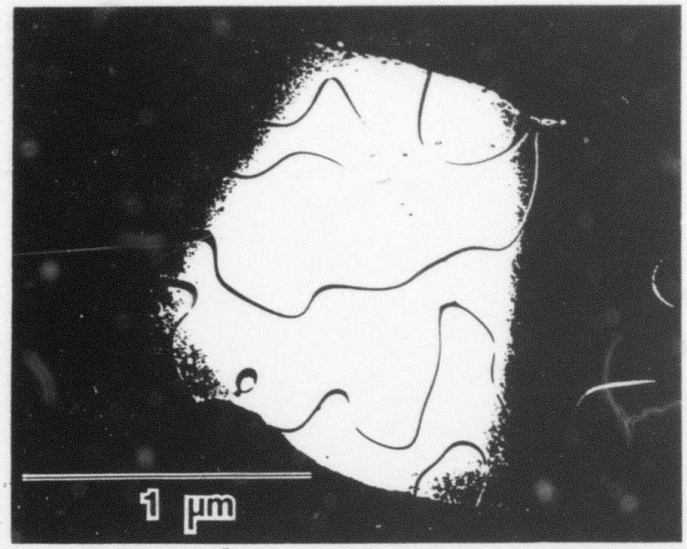

a

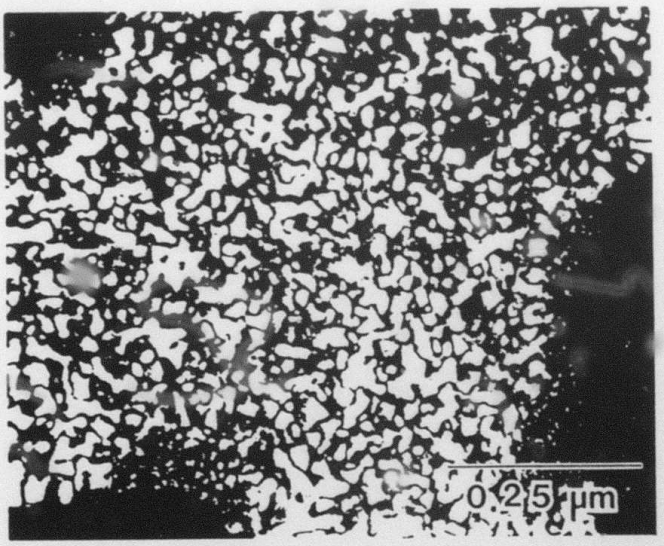

b

Figure 2 (a) (b). Dark field TEM micrographs using (111) $L2_1$ superlattice reflection of melt-spun ribbons of (a) Ni-25 at% Ti-25 at% Al and (b) Ni-37.5 at% Ti-12.5 at% Al.

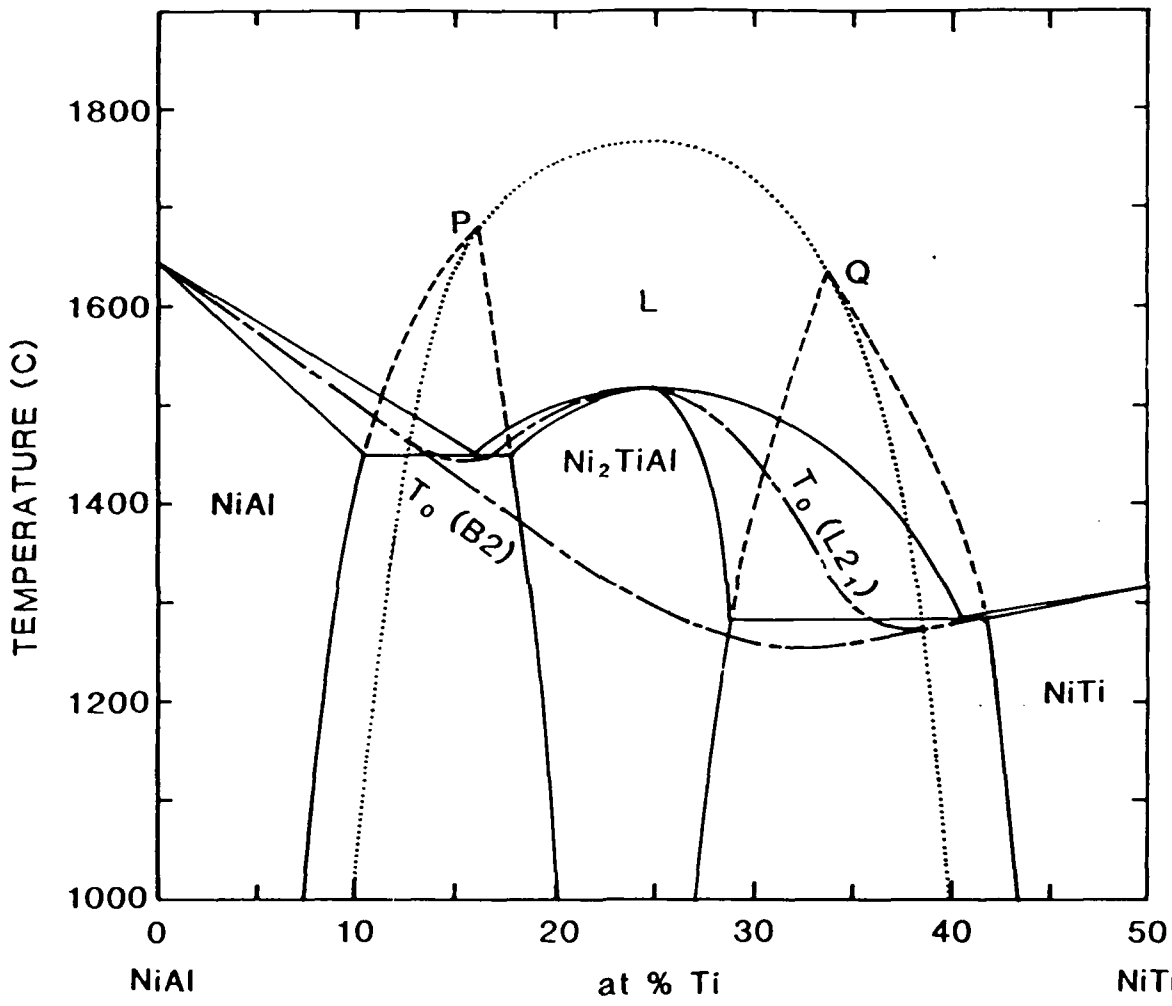

Figure 3. Estimated equilibrium phase ~~diagram~~ diagram (solid lines) for the NiAl-NiTi quasibinary system with schematic metastable boundaries and liquid-solid T_o curves. The dashed curves are the metastable extensions of the $L2_1$ + B2 two-phase fields. Points P and Q are the tricritical points. The dotted line is the B2 → $L2_1$ continuous ordering curve. The short-long dashed lines are the T_o curves.

Proceedings of RQ6, Montreal, August, 1987
to appear in Mat. Sci. and Eng.,1988

PATHWAYS FOR MICROSTRUCTURAL DEVELOPMENT IN TiAl

J. A. Graves*, L. A. Bendersky+, F. S. Biancaniello+,
J. H. Perepezko* and W. J. Boettinger+

+Metallurgy Division, Center for Materials Science
National Bureau of Standards, Gaithersburg, MD 20899

*Department of Metallurgical and Mineral Engineering
University of Wisconsin, Madison, WI 53706

Abstract

Rapid solidification processing (RSP) of intermetallic alloys can provide alternative solidification paths and lead to the formation of metastable products. For the intermetallic TiAl with an equilibrium $L1_0$ structure RSP has yielded a metastable hcp (α-Ti) phase in both fine powder and melt spun ribbon. Based upon TEM observations of a fine anti-phase domain structure the hcp phase orders to the Ti_3Al (DO_{19}) structure following solidification. A metastable phase diagram analysis indicates that a melt undercooling of about 100°C is required for partitionless formation of a hcp phase from an equiatomic melt and reveals other possible solidification pathways including the nucleation of metastable disordered bcc and fcc phases. Each of the potential pathways offers further opportunity for microstructural modification by solid state annealing treatments.

Introduction

Based upon the equilibrium phase diagram the opportunities for the solidification processing of intermetallic compounds appear to be quite limited. With conventional melt processing of

intermetallics one or more peritectic reactions and wide liquidus - solidus separation are encountered and lead to large-scale composition segregation which is difficult to eliminate during post-solidification treatments.

At the same time the characteristics which make intermetallics unattractive for conventional processing qualify them as suitable candidates for RSP. The high rate of heat extraction and rapid crystal growth rates commonly associated with RSP yield fine-scale microstructures with reduced segregation tendencies or metastable products (1). Indeed, a recent report on rapid solidification of TiAl alloy powders has demonstrated one of the alternate metastable solidification pathways involving the nucleation of a disordered hcp α-Ti phase (2). The current study represents a more detailed examination of RSP microstructures in TiAl.

Experimental Method

Alloys were arc melted in gettered argon from 99.9% pure components for three compositions: Ti-36 wt% Al, Ti-38wt% Al and Ti-40wt% Al. At elevated temperature at equilibrium these alloy compositions should be single phase TiAl (3). The composition Ti-38 wt% Al corresponds closely to the break in the liquidus for the peritectic reaction $L+\beta(Ti) \rightarrow TiAl$ at approximately 1480°C whereas Ti-40 wt% Al is in the field of primary crystallization of TiAl below approximately 1480°C.

Ribbons were prepared by melt spinning on a copper wheel in helium. Powders were produced by a rotating electrode process (4) under a helium atmosphere. Ribbon samples were prepared for

TEM examination by twin jet electropolishing in a 92% acetic acid and 8% perchloric acid electrolyte at room temperature. Internal sections were etched with Kroll's reagent.

Results

Powders

X-ray diffraction analysis of the finest powder size fraction revealed the presence of two crystal structures: the equilibrium TiAl, $L1_0$ phase and a metastable hexagonal structure which was indexed according to the ordered Ti_3Al (DO_{19}) α_2 phase (5). As shown in Fig. (1) the finest powder was comprised predominantly of the α_2 phase, with only a minor fraction of the total volume (<10%) represented by TiAl. The relative abundance of the two phases varied with powder size, with the metastable product decreasing in amount as the particle size increased. Microstructural examination of the fine powder revealed that approximately 30% of the particles were single phase while the remainder were dual phase. The morphology of the dendritic structure in dual phase powders, as illustrated in Fig. 2, showed a consistent tendency for primary arms to have a six-fold rotational symmetry, with secondary arms maintaining growth angles of approximately 60° with respect to primary dendrite arms. This growth pattern is indicative of a hcp structure (6) for which the preferred growth directions are of the <10$\bar{1}$0> type (6). Thus, solidification of the finest powder occurred by the formation of a hcp structure from the melt. Droplets which nucleate at reduced undercoolings form an initial single phase hcp region, however, as recalescence raises the particle

temperature, a two-phase structure develops having a dendritic hcp phase with TiAl in the interdendritic regions. Ordering in the solid state to the α_2 structure can occur as the hcp phase cools.

Ribbons

The as-solidified microstructures of the Ti-38 wt% Al and Ti-40 wt% Al alloys after melt spinning are very similar and can be seen in Fig. 3. The dark regions tend to be convex, suggesting that this phase forms from the melt first, and share a common crystallographic orientation. These regions were identified as the hexagonal DO_{19} structure by convergent beam electron diffraction (CBED) as shown in Fig. 4a, while the phase shown in light contrast in Fig. 3 is identified in Fig. 4b as having the tetragonal $L1_0$ (TiAl) structure. The DO_{19} phase contains a fine distribution of antiphase domains which are shown in dark field in Fig. 5 using a superlattice reflection. These fine antiphase domains indicate that the DO_{19} order was established in the solid state from a disordered HCP phase originally produced from the melt which is consistent with the observations of dendrite morphology in powders.

Thermal Stability

To assess the thermal stability of the metastable α_2 structure the finest powder for the Ti-36 wt% Al alloy was subjected to a controlled heating cycle during x-ray diffraction under a helium atmosphere, Fig. 1. Significant decomposition of the metastable α_2 phase begins at temperatures above 500°C, with the transformation to TiAl being completed at approximately

700°C. The microstructural changes during decomposition that are illustrated in Fig. 6 revealed a plate-like morphology within the α_2 phase consisting of alternating parallel plates of α_2 and TiAl. In some regions of the as-solidified ribbons, the DO_{19} phase has begun to decompose by the same mechanism. With continued annealing the TiAl plates thicken at the expense of α_2. This pattern resembles very closely the mirostructural morphology that develops in cobalt during the FCC $\updownarrow$ HCP transformation (7). Indeed from TEM analysis the orientation relationship between the phases confirms that reported by Blackburn (8) as:

$$(0001)_{DO_{19}} \;||\; (111)_{L1_0}$$
$$[2\bar{1}\bar{1}0]_{DO_{19}} \;||\; \langle 110\rangle_{L1_0}$$

so that the decomposition of α_2 to TiAl represents the ordered phase counterpart to the allotropic transformation in cobalt. The observed crystallography indicates a low index relationship and a low mobility for the α_2/γ transformation interface and is consistent with the relatively wide temperature range for the decomposition of α_2 in TiAl.

Discussion

The microstructural development that has been observed following rapid solidification of TiAl alloys identifies one metastable pathway for processing reactions. For both melt spun ribbon and powder the pathway begins with the solidification of disordered hcp α-Ti phase from an undercooled liquid, with the

interdendritic regions solidifying as a $L1_0$ TiAl phase. Rapid solid state transformations change the hcp into the DO_{19} structure during quenching. Because the DO_{19} is supersaturated with respect to the $L1_0$ phase, solid state decomposition proceeds with the DO_{19} phase transforming into a mixture of alternating, parallel plates of DO_{19} and $L1_0$ phases and by thickening of the plates to a single phase $L1_0$.

In evaluating potential rapid solidification pathways and phase selection, metastable phase diagrams together with the relevant T_0 curves provide valuable guidance (9,10). For the Ti-Al alloy system, T_0 curves can be calculated using thermodynamic data supplied by Murray (3) for the bcc and hcp product structures, as illustrated in Fig. 7. Based upon these T_0 curves an equiatomic alloy would require an undercooling of only about 100°C to provide a driving force for formation of the hcp solid from the melt. It is interesting to note, however, that at the equiatomic composition the $L1_0$ and bcc solids have T_0 temperatures above that of the hcp phase. This indicates the importance of kinetics in controlling product phase selection in an undercooled melt. As the Al content is increased beyond the equiatomic composition, or fcc-based ordered phases or a disordered fcc phase can become more favored among the metastable products from a driving force (i.e. undercooling) standpoint. A complete analysis of alternative solidification pathways (11) would include other product structures involving both disordered and ordered phases such as a CsCl ordered structure. Overall, it

is clear that rapid solidification can offer several intriguing microstructural options different from conventional casting for the processing of high temperature ordered intermetallic alloys.

Acknowledgement

The support of ARO (DAAL03-86-K-0164) and DARPA/URI (N0014-86-K-0753/P.O. No. VB38640-0) for JAG and JHP and DARPA (6065) for LAB, FSB and WJB for the study of intermetallic compounds is gratefully acknowledged.

References

1. C. C. Koch, Mat. Res. Soc. Symp. Proc. 39, 397 (1985).
2. J. A. Graves, J. H. Perepezko, C. H. Ward and F. H. Froes, Scripta Met. 21, 567 (1987).
3. J. L. Murray, submitted to Met. Trans.
4. E. J. Kosinski, "Progress in Powder Met." 38, Ed. by J. G. Bewley and S. W. McGee, MPIF/APMI, Princeton, NJ (1982) p. 491.
5. A. J. Goldak and J. G. Parr, Trans. Met. Soc. AIME 221, 639 (1961).
6. B. Chalmers, "Principles of Solidification", John Wiley & Sons, N.Y., 117 (1964).
7. E. Votava, Acta Met. 8, 901 (1960).
8. M. J. Blackburn, "The Science, Technology and Application of Titanium", R. J. Jaffee and N. E. Promisel, Eds., Pergamon Press (Edinburgh, UK) 633 (1970).
9. J. H. Perepezko and W. J. Boettinger, Mat. Res. Soc. Symp. Proc., 19, 223 (1983).

10. W. J. Boettinger and J. H. Perepezko, "Rapidly Solidified Crystalline Alloys", S. K. Das, B. H. Kear and C. M. Adam, Eds. (TMS-AIME, Warrendale) 21 (1985).

11. L. A. Bendersky, J. A. Graves, J. H. Perepezko and W. J. Boettinger, to be published.

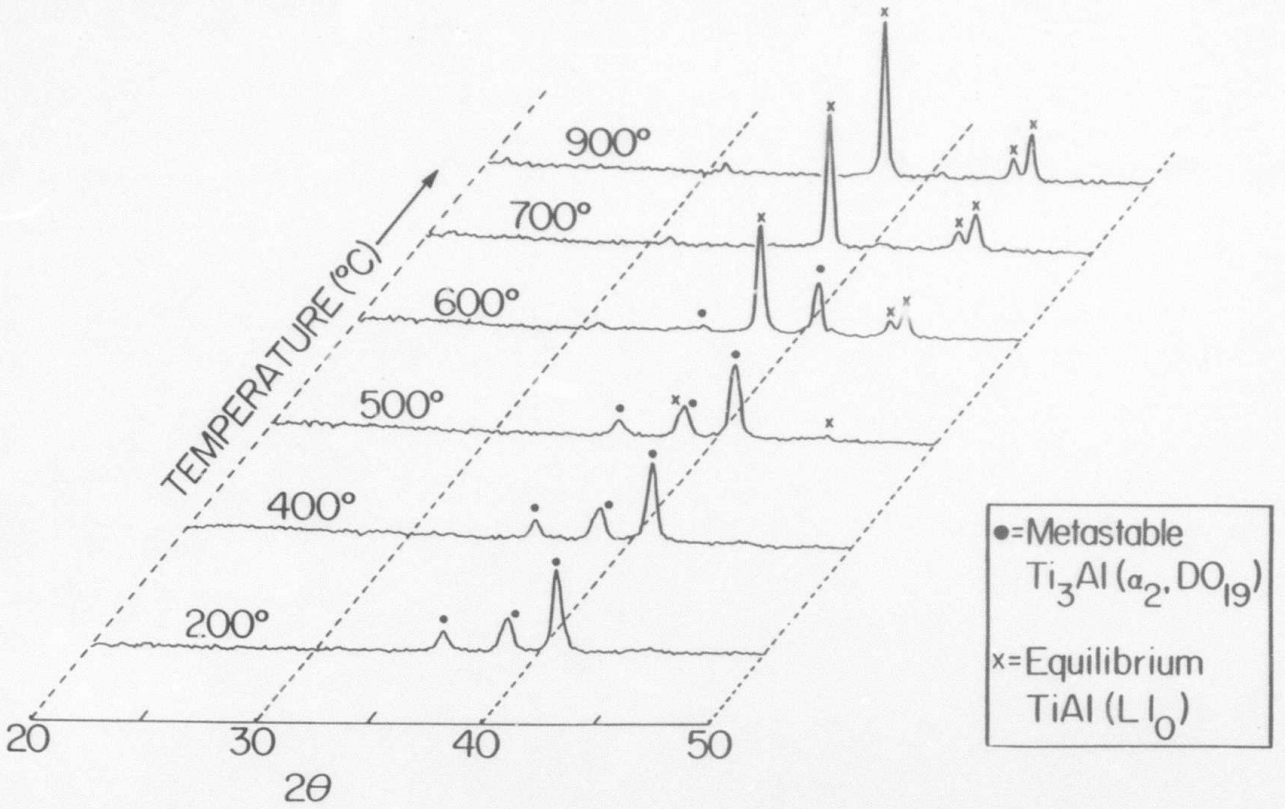

Fig.1. X-ray diffraction patterns showing decomposition of metastable (DO_{19}) structure to equilibrium ($L1_0$) phase in -44 micron powder during step scan annealing at indicated temperatures.

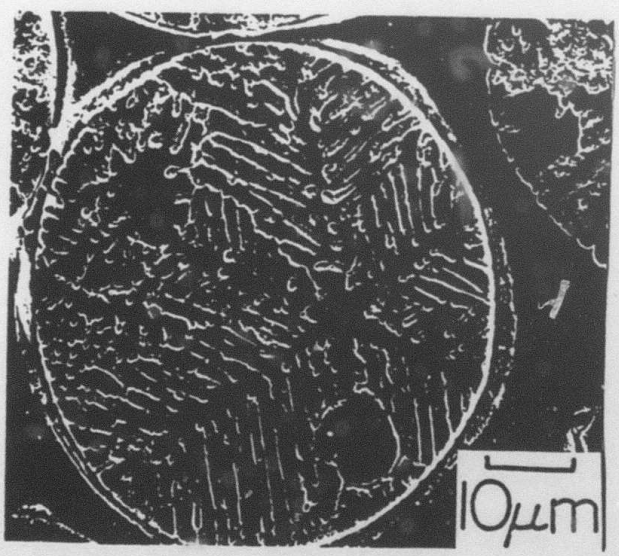

Fig. 2. Ti-36wt% Al particle showing HCP growth morphology.

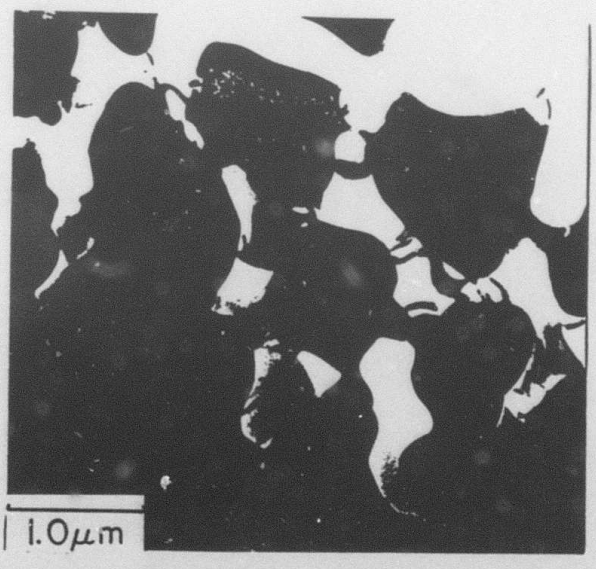

Fig. 3. As solidified microstructure of Ti-40wt% Al melt spun ribbon.

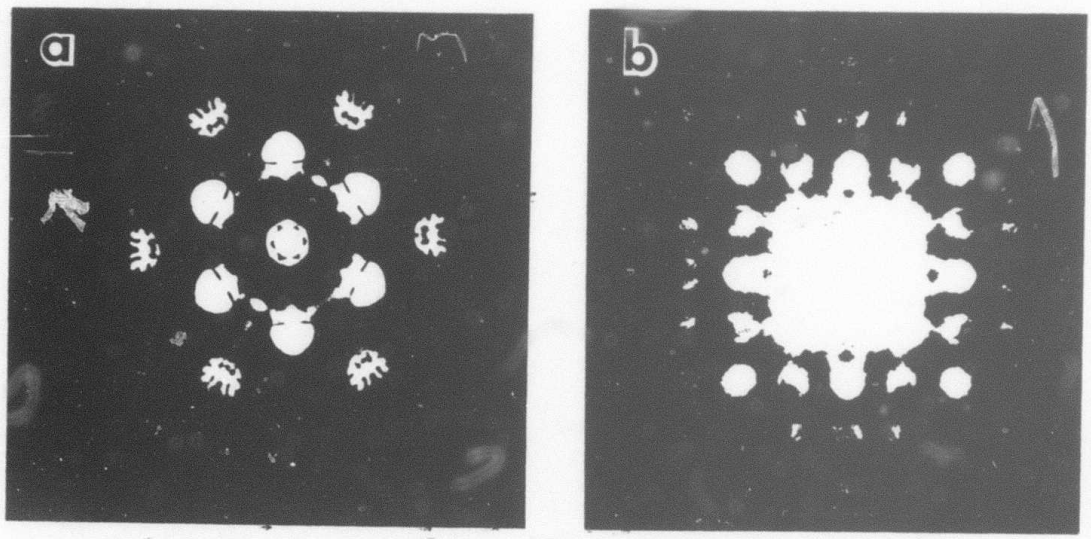

Fig. 4. CBED patterns identifying the (a) [0001] zone axis of the DO_{19} structure and (b) [001] zone axis of the $L1_0$ structure in Ti-40wt% Al melt spun ribbon.

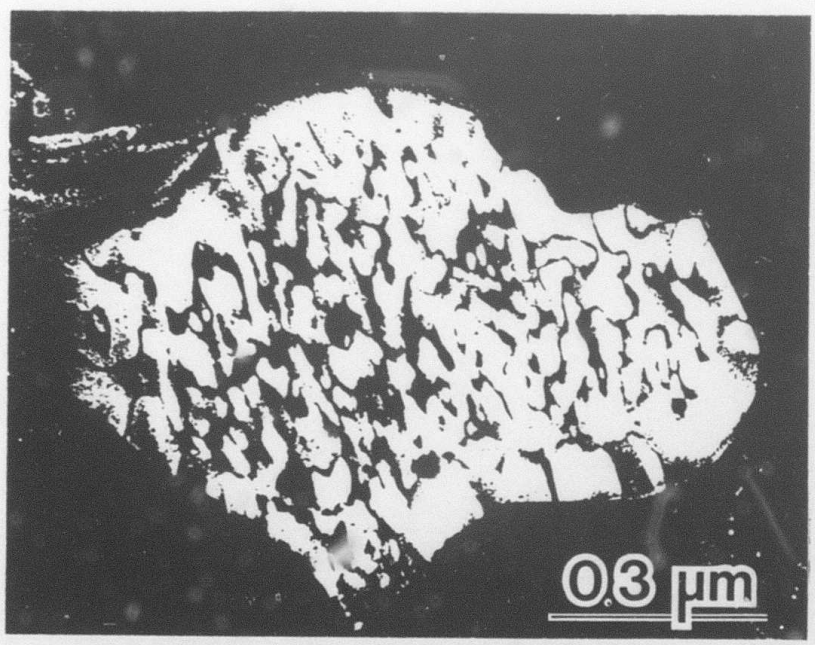

Fig. 5. Dark field image of the DO_{19} phase using a superlattice reflection. Note fine antiphase domains.

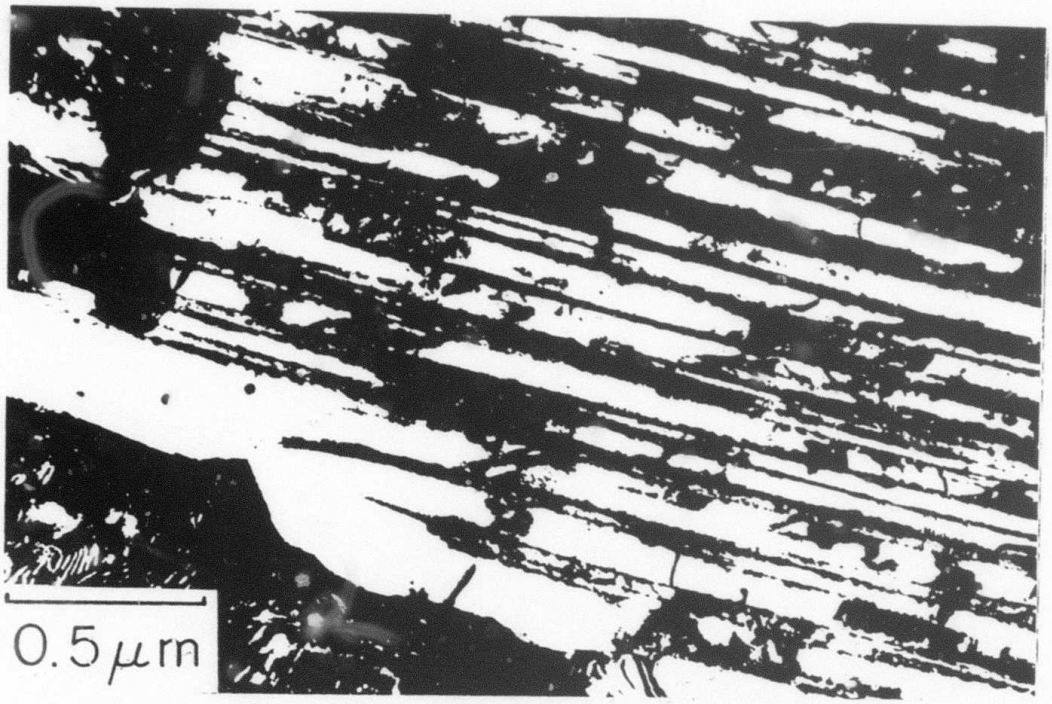

Fig. 6. Alternating plate structure of DO_{19} and $L1_0$ phases in melt spun Ti-40wt% Al ribbon.

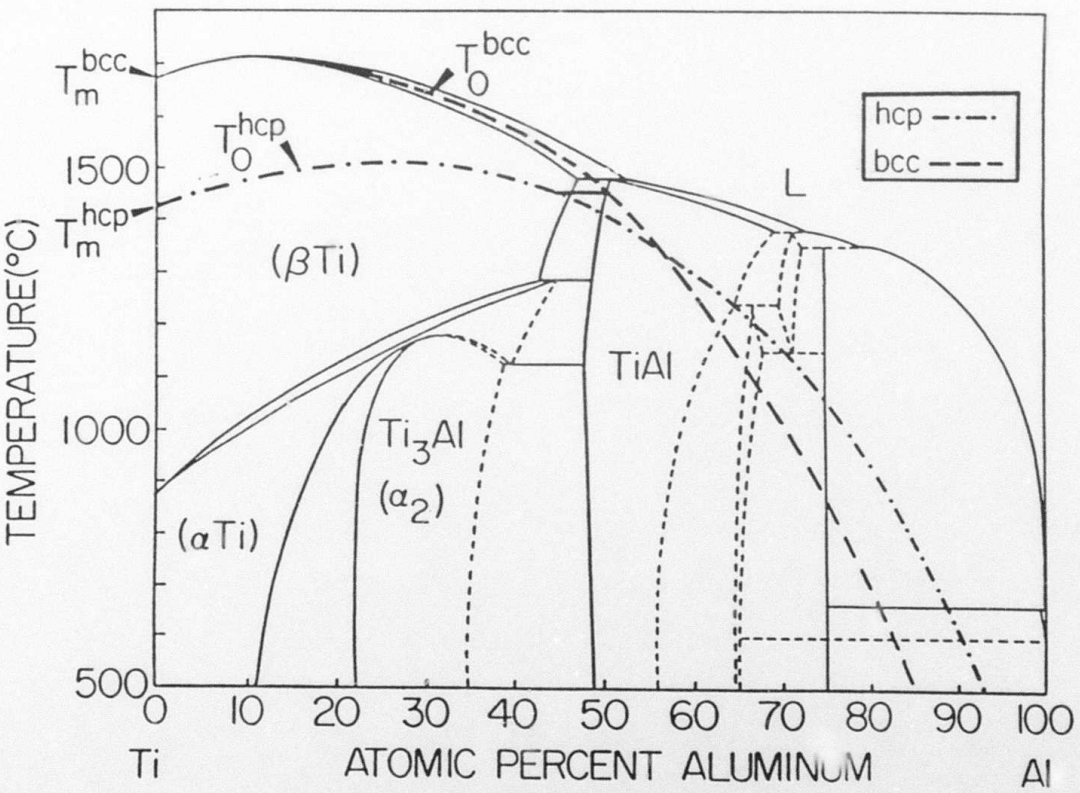

Fig. 7. Ti-Al phase diagram showing equilibrium phase fields and calculated T_0 curve estimates for BCC and HCP structures (3).